2017

Wave Profile for Breakdown Waves with a Large Current Behind the Wave Front

M. Hemmati
Arkansas Tech University, mhemmati@atu.edu

J. Griffiths
Arkansas Tech University

M. Bowman
Arkansas Tech University

Follow this and additional works at: http://scholarworks.uark.edu/jaas

 Part of the Physical Sciences and Mathematics Commons

Wave Profile for Breakdown Waves with a Large Current Behind the Wave Front

M. Hemmati, J. Griffiths, and M. Bowman

Department of Physical Sciences, Arkansas Tech University, Russellville, AR 72801, USA

*Correspondence: mhemmati@atu.edu

Running Title: Wave Profile for Breakdown Waves with a Large Current Behind the Wave Front

Abstract

For analytical solution of breakdown waves with a large current behind the wave front, we employ a one-dimensional, steady-state, three-component (electrons, ions, and neutral particles) fluid model. This project involves breakdown waves propagating in the opposite direction of the electric field force on electrons, anti-force waves (return stroke in lightning); and the electron gas partial pressure is considered to provide the driving force for the propagation of the wave. The basic set of equations consists of the equation of conservation of mass flux, equation of conservation of momentum, equation of conservation of energy, plus Poisson's equation. The waves are considered to have a shock front. In this study, we examine the possibility and validity of large currents measured and reported by few investigators. Existence of a relationship between wave speed and peak current values is investigated as well.

Existence of a large current behind the wave front alters the equation of conservation of energy and Poisson's equation, as well as the shock boundary condition on electron temperature. Considering a current behind the shock front, we have made appropriate modifications in our set of electron fluid dynamical equations. Using the modified set of equations and the shock condition on electron temperature, we have been able to integrate the set of electron fluid dynamical equations for current bearing anti-force waves. For a range of wave speeds and with the largest current possible for a specific wave speed, we present the wave profile for electric field, electron velocity, and the ionization rate within the dynamical transition region of the wave for anti-force waves.

Introduction

In the late 17th to early 18th century, scientists discovered a phenomenon in which mercury gives off a glow when shaken in an evacuated glass vessel. Hauksbee (1705) was among the first to examine closely the occurrence of such luminous pulses in evacuated containers and in 1705 was able to recreate and experiment with these pulses, but focused mostly on the effects of air pressure with little regard to electrical effects. Thomson (1893) observed a moving luminous pulse in an evacuated chamber and estimated that it moved at about half the speed of light. Observations made by Beams (1930) supported this estimation. Beams explained that this phenomenon arose from the conductivity of the gas behind the pulse and that this conductivity allows the pulse to carry a potential.

In later experiments Beams, Snoddy, and Dietrich (1936) were able to find how the velocity and form of the wave varied with applied potential and air pressure. They also found that it took longer for the initial wave to propagate from the electrode to ground than for the return wave that followed to get from ground to the electrode.

Schonland (1950) made progress on determining the speed of lightning pilot streamers, though the conditions of lightning discharges differ from those in evacuated chambers. Loeb (1965) worked on corona discharge, a similar phenomenon to breakdown waves in evacuated tubes, led to further progress in understanding the propagation of such waves.

Loeb's (1965) model involves excited-state atoms emitting photons as well as the excitation of new atoms, which will in turn emit photons, continuing the process. Later this model proved not to be accurate. Observations from experiments done by Fowler and Hood (1962) with higher velocity shock waves led to a mathematical model based on fluid dynamical equations. This model led Paxton and Fowler (1962) to a theory of breakdown wave propagation in which the wave front is an electron shock wave and the partial pressure of electron gas is the primary source of motion. Their model explains wave velocity and the effects of electric fields on wave propagation in positive and negative directions.

A convention was adopted by Paxton and Fowler (1962) that separated the electron fluid dynamical waves into two different types of waves. According to this convention, if the direction of the electric field force on

M. Hemmati, J. Griffiths, and M. Bowman

electrons is in the opposite direction of wave propagation, the wave is designated to be an antiforce wave. Conversely, if the direction of the electric field force on electrons is in the same direction as the wave propagation, the wave is referred to as a proforce wave. Paxton and Fowler (1962), proposed existence of two distinct regions in breakdown waves.

The two regions of the wave are the Debye sheath layer, a thin section directly behind the shock front, where in antiforce waves, the electric field reaches a maximum but falls to a negligible value, and a thicker quasi-neutral region that comes after the Debye sheath. In this quasi-neutral region the electron gas temperature is decreased due to continued ionization while the ion and electron densities come to equilibrium.

With the two distinct categories of waves and the two regions being known, Shelton and Fowler (1968) modeled the proforce wave mathematically. This model assumes a condition of zero current behind the shock front of the breakdown wave. Fowler et al. (1984), trying to integrate the set of electron fluid-dynamical equations with the aim of meeting the physically accepted conditions at the trailing edge of the sheath region, investigated numerous approximations for the proforce wave case. This analysis led them to the conclusion that a heat conduction term must be incorporated into the conservation of energy equation. The group also concluded that there was a discontinuity in the temperature derivative at the shock front of the wave. Elastic collisions between heavy particles and electrons were also found to be resulting in a loss of energy for the electrons.

To derive their set of electron fluid-dynamical equations Shelton and Fowler (1968) considered the net current behind the shock front to be zero. This is known as the zero current condition:

$$e(N_i V - nv) = 0$$

where e, N_i, V, n, and v are the charge of an electron, ion number density inside the sheath region, wave velocity, electron number density, and electron velocity, respectively. Fowler et al. (1984) developed equations for the conservation of mass, momentum and energy coupled with Poisson's equation for the proforce wave case. These equations are:

$$\frac{d(nv)}{dx} = n\beta, \qquad (1)$$

$$\frac{d}{dx}[mnv(v - V) + nkT_e] = -enE$$
$$-Kmn(v - V), \qquad (2)$$

$$\frac{d}{dx}[mnv(v - V)^2 + nkT_e(5v - 2V) + 2env\phi$$
$$-\frac{5nk^2 T_e}{mK}\frac{dT_e}{dx} = -3\left(\frac{m}{M}\right)nkKT_e -$$
$$\left(\frac{m}{M}\right)Kmn(v - V)^2, \qquad (3)$$

$$\frac{dE}{dx} = \frac{e}{\varepsilon_o}(N_i - n), \qquad (4)$$

in these equations, E, x, β, K, V, M, E_o, k and Φ are the electric field and position in the wave profile, ionization frequency, elastic collision frequency, wave velocity, neutral particle mass, electric field at the wave front, Boltzmann's constant and ionization potential respectively. Also m and T_e are electron mass and electron gas temperature respectively. With the assumption that the net current behind of the wave front is zero, equation (4) reduces to

$$\frac{dE}{dx} = \frac{e}{\varepsilon_0}n\left(\frac{v}{V} - 1\right). \qquad (5)$$

Fowler et al. (1984) applied a set of non-dimensional variables to the set of electron fluid dynamical equations to reduce the set to non-dimensional form. The variables are:

$$\omega = \frac{2m}{M}, \quad \kappa = \frac{mVK}{eE_o}, \quad \mu = \frac{\beta}{K},$$

$$\alpha = \frac{2e\phi}{mV^2}, \quad \psi = \frac{v}{V}, \quad \nu = \frac{2e\phi n}{\varepsilon_o E_o^2},$$

$$\theta = \frac{T_e k}{2e\phi}, \quad \eta = \frac{E}{E_o}, \quad \xi = \frac{xeE_o}{mV^2}$$

Where, the dimensionless variables ν, ψ, θ, μ, η and ξ are defined as electron number density, electron velocity, electron temperature, ionization rate, net electric field, and position inside the sheath region of the wave, respectively. α and κ represent wave parameters. Therefore, in dimensionless form, the complete set of equations for the proforce case are

$$\frac{d}{d\xi}[\nu\psi] = \kappa\mu\nu, \qquad (6)$$

$$\frac{d}{d\xi}[\nu\psi(\psi - 1) + \alpha\nu\theta] = -\nu\eta - \kappa\nu(\psi - 1), \qquad (7)$$

$$\frac{d}{d\xi}\left[\nu\psi(\psi-1)^2 + \alpha\nu\theta(5\psi-2) + \alpha\nu\psi + \frac{5\,\alpha^2\nu\theta}{\kappa}\frac{d\theta}{d\xi}\right] = -\,\omega\kappa\nu[3\alpha\theta + (\psi-1)^2] \qquad (8)$$

$$\frac{d\eta}{d\xi} = \frac{\nu}{\alpha}(\psi-1). \qquad (9)$$

With the proforce wave case equations completed and solved, attention shifted to the antiforce case. However, there were many problems in formulating a set of equations for antiforce waves similar to the set of equations describing proforce waves. To apply the set of electron fluid-dynamical equations to antiforce waves, modification of the equations is required. Additional changes must be considered and modifications must be made to the non-dimensional variables used in the proforce case in order for application to the antiforce case to be accurate.

In order for the set of electron fluid dynamical (EFD) equations to be non-dimensional, the following dimensionless variables were derived by Hemmati (1999) to the EFD equations (1-3, 5):

$$\omega = \frac{2m}{M}, \quad \kappa = -\frac{mVK}{eE_o}, \quad \mu = \frac{\beta}{K},$$

$$\alpha = \frac{2e\phi}{mV^2}, \quad \psi = \frac{v}{V}, \quad \nu = \frac{2e\phi n}{\varepsilon_o E_o^2},$$

$$\theta = \frac{T_e k}{2e\phi}, \quad \eta = \frac{E}{E_o}, \quad \xi = -\frac{xeE_o}{mV^2}$$

It was previously assumed by Sanmann and Fowler (1975) that μ, the ionization rate, was purely a function of θ, electron temperature. Fowler et al. (1984) concluded that this was not the case. In fact, calculating the ionization rate within the sheath region of the wave, random and directed electron motions must be taken into account. Shelton assumed that μ was constant and it would later be determined by Fowler et al. (1984) that the ionization rate does indeed remain substantially constant near the front of the sheath region, though it changes later. It was thought by Shelton that heat conduction was negligible in the sheath region and throughout the quasi-neutral region. It was determined by Fowler et al. (1984) that this was an error in the formulation of the equations and a term for heat conduction was included in the equations.

In the laboratory frame, ion motion is considered negligible due to the fact that no Doppler shift has been observed in the analysis of radiation emitted from the propagation of breakdown waves. In the wave frame, heavy particles will be moving in the negative x direction. Therefore, heavy particle speed, *V*, is negative, while E_0 is positive, κ and ξ are therefore both negative.

After applying these dimensionless variables, the EFD equations (1-3, 5) become the non-dimensional set of equations describing the antiforce wave case. The following equations are the complete set of non-dimensional EFD equations developed by Hemmati (1999) for the antiforce wave:

$$\frac{d}{d\xi}[\nu\psi] = \kappa\mu\nu, \qquad (10)$$

$$\frac{d}{d\xi}[\nu\psi(\psi-1) + \alpha\nu\theta] = \nu\eta - \kappa\nu(\psi-1), \qquad (11)$$

$$\frac{d}{d\xi}\left[\nu\psi(\psi-1)^2 + \alpha\nu\theta(5\psi-2) + \alpha\nu\psi - \frac{5\,\alpha^2\nu\theta}{\kappa}\frac{d\theta}{d\xi}\right] = 2\nu\eta(\psi-1) - \omega\kappa\nu[3\alpha\theta + (\psi-1)^2], \qquad (12)$$

$$\frac{d\eta}{d\xi} = -\frac{\nu}{\alpha}(\psi-1). \qquad (13)$$

Letting I_1 represent the current behind the wave front we get

$$I_1 = eN_iV_i - env. \qquad (14)$$

Solving for N_i gives

$$N_i = \frac{I_1}{eV} + \frac{nv}{V}. \qquad (15)$$

Substituting this in equation (4) results in

$$\frac{dE}{dx} = \frac{e}{\varepsilon_0}\left(\frac{I_1}{eV} + \frac{nv}{V} - n\right). \qquad (16)$$

Substituting the dimensionless variables in previous equation results in

$$\frac{d\eta}{d\xi} = \frac{\kappa I_1}{\varepsilon_0 K E_0} - \frac{\nu}{\alpha}(\psi-1). \qquad (17)$$

Finally, letting ι be the dimensionless current representation of $\frac{I_1}{\varepsilon_0 K E_0}$ gives

$$\frac{d\eta}{d\xi} = \kappa\iota - \frac{\nu}{\alpha}(\psi-1). \qquad (18)$$

Equation (18) can be solved for $v(\psi - 1)$ and the result can be substituted into equation (12) giving the final form of the conservation of energy equation.

The preceding equations derived by Hemmati et al (2011) give us our final form of the EFD equations for antiforce waves:

$$\frac{d}{d\xi}[v\psi] = \kappa\mu v, \qquad (19)$$

$$\frac{d}{d\xi}[v\psi(\psi - 1) + \alpha v\theta] = v\eta - \kappa v(\psi - 1), \qquad (20)$$

$$\frac{d}{d\xi}\left[v\psi(\psi - 1)^2 + \alpha v\theta(5\psi - 2) + \alpha v\psi - \frac{5\alpha^2 v\theta}{\kappa}\frac{d\theta}{d\xi} + \alpha\eta^2\right] = 2\eta\kappa\alpha - \omega\kappa v[3\alpha\theta + (\psi - 1)^2], \qquad (21)$$

$$\frac{d\eta}{d\xi} = \kappa\iota - \frac{v}{\alpha}(\psi - 1). \qquad (22)$$

All quantities in this set of equations are intrinsically positive, including, κ. Equations (19-22) describe the final set of EFD equations with a large current behind the wave front for antiforce waves.

It was assumed by Shelton and Fowler (1968) that ionization rate was constant, and then later thought by Sanmann and Fowler (1975) to be a function of electron temperature only. A study by Fowler (1983) showed that in the calculation of ionization rate, ionization from both random and directed electron motion must be considered. Therefore, we have used an expression derived by Fowler (1983) to calculate the ionization rate within the sheath region of the wave that takes into account ionization from both directed and random electron motions. Thus,

$$\mu = \mu_0 \int_{\frac{1}{\sqrt{2\theta}}}^{\infty} \sigma_i z^2 dz \int_B^{\infty} \frac{e^{-(z-u)^2} - e^{-(z+u)^2}}{u} du\, e^{-2Cu}$$

where $B = (1 - \psi)/\sqrt{2\alpha\theta}$ and $C = \kappa\sqrt{2\alpha\theta}/\eta$.

Results and Discussion

Uman et al. (2000) reported return stroke wave speeds as low as 0.46×10^8 m/s. Similarly, Rakov (2000) in his study of positive and bipolar lightning discharges measured a range of wave-speeds in agreement with other experimental works. His reported wave speed values were between 0.3×10^8 m/s $- 1.7 \times 10^8$ m/s. Rakov (2000) also reported in the study of the characteristics of positive and bipolar lightning that the

return stoke current ranged from 10 kA – 40 kA depending upon experimental location. While studying rocket triggered lightning strokes, Wang et al. (1999) observed a peak current value of around 12 kA – 21 kA. During the investigation of the time derivative of the electric field in triggered lightning strokes, Uman et al. (2000) observed current values for return stokes as large as 30.4 kA.

For lightning return strokes, the current values generally reported by investigators lie within the range of 10-40 kA. However, few investigators report existence of currents as high as 300 kA (Rakov, 2000).

A trial and error method was used to integrate equations (19 – 22) through the sheath region of the wave. The largest current, ι, that led to successful solutions was chosen for given wave speeds, α, and values for the wave constant, κ, electron velocity, ψ, and electron number density, v, were chosen so that integration of the set of equations led to a conclusion consistent with the expected conditions at the trailing edge of the sheath. This was done by repeatedly adjusting κ, ψ, and v until integration led to results that were in agreement with the expected conditions at the end of the dynamical transition region of the wave.

Certain boundary conditions must be met in order for integration to be successful. Namely, η_2, the electric field at the end of the sheath region, must approach 0 and, ψ_2, the dimensionless electron velocity at the end of the sheath region, must approach 1.

The following initial variable values lead to successful integration of the set of electron fluid dynamical equations and were found to satisfy the boundary conditions at the end of the sheath region of the wave:

$\alpha = 0.001$, $\iota = 7$, $\kappa = 0.144$, $\psi_1 = 0.4721$, $v_1 = 0.2161$

$\alpha = 0.01$, $\iota = 5$, $\kappa = 0.13$, $\psi_1 = 0.7$, $v_1 = 0.7696$

$\alpha = 0.1$, $\iota = 1$, $\kappa = 0.44$, $\psi_1 = 0.8321$, $v_1 = 0.71$

$\alpha = 1$, $\iota = 0.25$, $\kappa = 0.18$, $\psi_1 = 0.75$, $v_1 = 0.7$

In figure 1 the electric field intensity, η, is shown as a function of the electron velocity, ψ. The gaps in the curves $\alpha = 0.001$ and $\alpha = 0.01$ are due to the fact that only one out of ten data points calculated were plotted. In this figure we can clearly see that the electric field is falling to 0 and the electron velocity is approaching 1, which satisfies the conditions at the trailing edge of the wave.

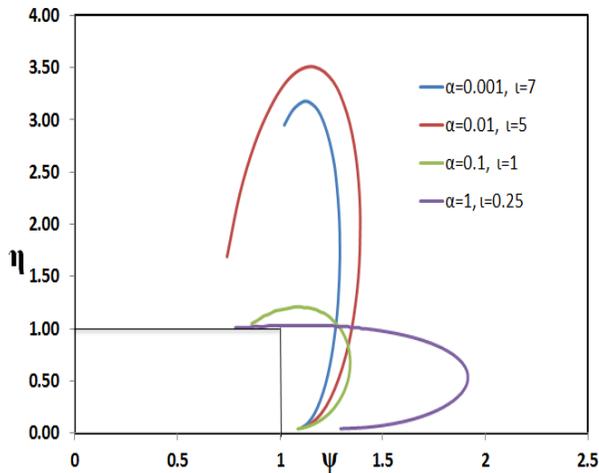## Wave Profile for Breakdown Waves with a Large Current Behind the Wave Front

Figure 1: Dimensionless electric field, η, as a function of dimensionless electron velocity, ψ, within the sheath region of the wave.
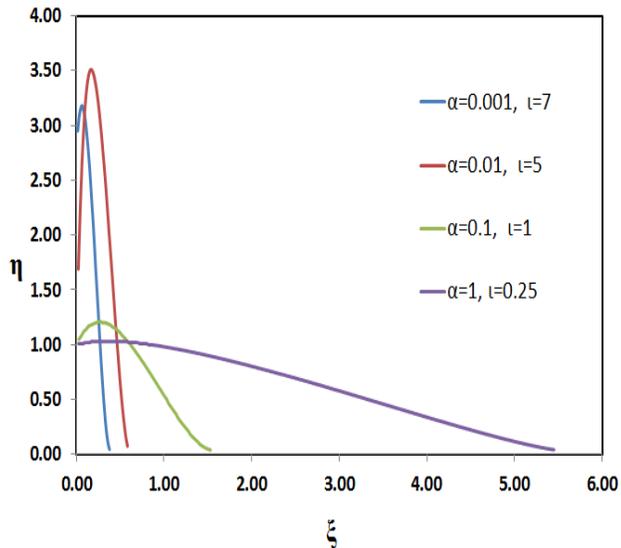
within the sheath region of the wave. To reduce the computation time, ionization rate was kept constant for ten integration steps and calculated every tenth step. To keep track of variable changes while integration and computation occur, only every tenth integration step is printed so that all previous data lines can be displayed simultaneously on the computer screen. Therefore, regarding change in ionization rate, every hundredth integration step is displayed. The sharp changes in the graphs are an unavoidable consequence of keeping the ionization rate constant and displaying the change in ionization rate only every hundredth step. Shelton and Fowler (1968) assumed that the ionization rate would remain constant through the sheath region of the wave. We see here that ionization rate remains constant for a short time behind the wave front, but generally changes as we move through the sheath region of the wave.
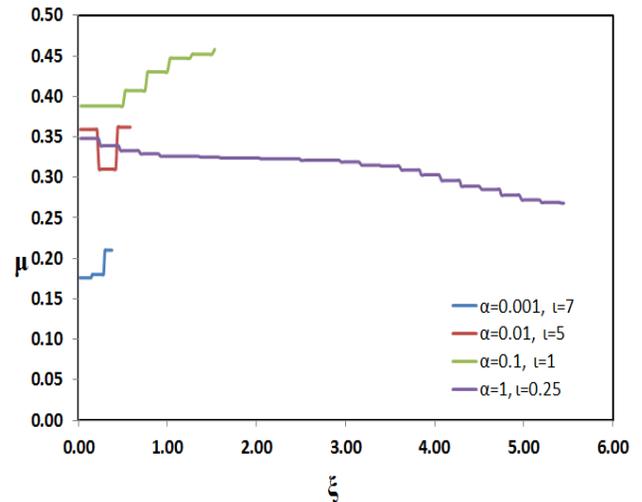

Figure 2: Dimensionless electric field, η, as a function of position, ξ, within the sheath region of the wave.

Figure 3: Dimensionless ionization rate, μ, as a function of position, ξ, within the sheath region of the wave.

In figure 2 the electric field intensity, η, is shown as a function of the position, ξ, within the sheath region of the wave. The fall of the electric field to zero marks the end of the sheath region of the wave. Sanmann and Fowler (1975) applied fluid dynamic techniques to antiforce waves and for a wave speed of 10^7 m/s found a total sheath thickness of 0.5 m. Fujita et al. (2003), in measuring electron densities behind shock waves, reported a sheath thickness of 0.05 m. Our data for ξ for waves at speeds of 3 X 10^7 m/s show a sheath thickness of 0.025 m.

In figure 3, the dimensionless ionization rate, μ, is shown as a function of the dimensionless position, ξ,

For return lightning strokes, some investigators have suggested the existence of a relationship between the peak current values and wave speed values (Wagner 1963); however, some others, (Willett et al. 1989), especially researchers investigating triggered lightning in Florida, disagree with the existence of such a relationship. For lightning return strokes, our solutions indicate, as the wave speed increases, the current values that it can support increases as well.

Conclusions

We have considered the existence of a large current behind the wave front and found a range of wave speeds and their corresponding maximum current values for

which integration of the electron fluid-dynamical equations led to results in agreement with the boundary conditions at the trailing edge of the sheath region. For lightning return strokes, our solutions also confirm the existence of large currents. Agreement between the results of the solutions of the electron fluid-dynamical equations with experimental evidence such as wave velocity and electron number density are conformations of the validity of the fluid model.

Acknowledgements

Literature Citeed

Beams JW. 1930. The propagation of luminosity in discharge tubes. American Physical Society Journal 36(5):997.

Beams JW, LB Snoddy, and **JR Dietrich.** 1936. The propagation of potential in discharge tubes. American Physical Society Journal 50(5):469.

Complete Dictionary of Scientific Biography. 2016. Hauksbee, Francis. Encyclopedia.com. Accessed on 21 Mar 2017.

Fowler RG. 1983. A trajectory theory of ionization in strong electric fields. Journal of Physics B. 16:4495.

Fowler RG and **JD Hood.** 1962. Very fast dynamical wave phenomenon. American Physical Society Journal 128(3):991.

Fowler RG, M Hemmati, RP Scott, and **S Parsenajadh.** 1984. Electric breakdown waves: Exact numerical solutions. Part I. The Physics of Fluids 27, 6:1521-26.

Hemmati M. 1999. Electron shock waves: Speed range for antiforce waves. Proceedings of 22nd International Symposium on Shock Waves. Pp. 995-1000.

Hemmati M, W Childs, H Shojaei and **D Waters.** 2011. Antiforce current bearing waves. Proceedings of 28th International Symposium on Shock Waves.

Loeb LB. 1965. Ionizing waves of potential gradient. Science 148(3676):1417.

Paxton GW and **RG Fowler.** 1962. Theory of breakdown wave propagation. Physics Review. 128(3):993-997.

Rakov VA. 2000. Positive and bipolar lightning discharges: a review. Proceedings of 25th International Conference on Lighting Protection. p103-108.

Sanmann E and **RG Fowler.** 1975. Structure of electron fluid dynamical plane waves: Antiforce waves. The Physics of Fluids 18(11):1433-1438.

Schonland BFJ. 1950. The flight of thunderbolts. Clarendon Press (Oxford). 152 p.

Shelton GA and **RG Fowler.** 1968. Nature of electron-fluid dynamical waves. The Physics of Fluids 11(4):740-746.

Thomson JJ. 1893. Notes on recent research in electricity and magnetism. Clarendon Press (Oxford). 600 p.

Uman MA, VA Rakov, KJ Schnetzer, JK Rambo, DE Crawford, and **RJ Fisher.** 2000. Time derivative of the electric field 10, 14, 30 m from triggered lightning strokes. Journal of Geophysical Research 105(D12):15,577-15,595.

Wagner CF. 1963. Relation between stroke current and velocity of return stroke. IEEE Transactions on Power Apparatus and Systems. 82:609-17.

Wang D, VA Rakov, MA Uman, N Takagi, T Watanabe, DE Crawford, KJ Rambo, GH Schnetzer, RJ Fisher, and **ZI Kawasaki.** 1999. Attachment process in rocket-triggered lightning strokes. Journal of Geophysical Research 104(D2):2143-50.

Willett JC, JC Bailey, VP Idone, A Eybert-Berared, and **L Barret.** 1989. Sub-microsecond inter-comparison of radiation fields and currents in triggered lightning return stroke based on the transmission-line. Journal of Geophysical Research. 94:13275-86.